ELSEVIER

Journal of Chromatography A, 795 (1998) 199–210

JOURNAL OF CHROMATOGRAPHY A

Direct measurements of convective fluid velocities in superporous agarose beads

Per-Erik Gustavsson[a], Anders Axelsson[b], Per-Olof Larsson[a,*]

[a]*Department of Pure and Applied Biochemistry, Center for Chemistry and Chemical Engineering, Lund University, P.O. Box 124, S-221 00 Lund, Sweden*

[b]*Department of Chemical Engineering 1, Center for Chemistry and Chemical Engineering, Lund University, P.O. Box 124, S-221 00 Lund, Sweden*

Received 21 May 1997; received in revised form 9 September 1997; accepted 11 September 1997

Abstract

Superporous agarose beads contain two sets of pores, diffusion pores and so-called superpores or flow pores, in which the chromatographic flow can transport substances to the interior of each individual bead [Gustavsson and Larsson, J. Chromatogr. A 734 (1996) 231]. The existence of pore flow may be proven indirectly by the chromatographic performance of beads but it has never been directly demonstrated in a chromatographic bed. In this report, pore flow was directly measured by following the movement of micro-particles (dyed yeast cells) in a packed bed. The passage of the micro-particles through the superpores and through the interstitial pores was followed by a microscope/video camera focused on beads which were situated four layers from the glass wall. The video recordings were subsequently used to determine the convective fluid velocities in both the superpores and the interstitial pores. Experiments were carried out with three different bead size ranges, all of which contained superporous beads having an average superpore diameter of 30 μm. The superpore fluid velocity as % of interstitial fluid velocity was determined to be 2–5% for columns packed with 300–500-μm beads (3% average value), 6–12% for columns packed with 180–300 μm beads (7% average value) and 11–24% for columns packed with 106–180-μm beads (17% average value). These data were compared to and found to agree with theoretically calculated values based on the Kozeny–Carman equation. In order to observe and accurately measure fluid velocities within a chromatographic bed, special techniques were adopted. Also, precautions were made to ensure that the experimental conditions used were representative of normal chromatography runs.

Keywords: Superporous agarose beads; Convective fluid velocity; Stationary phases, LC; Agarose

1. Introduction

In the last few years, new types of packing materials for column chromatography have emerged which offer improved mass transfer properties that can be ascribed to intraparticle convection [1–5]. The theoretical aspects of intraparticle convection as applied to catalysts [6–8] and chromatographic supports [5,9–13] have been investigated by several groups. Recently, a new type of support material, so-called superporous agarose [14,15], was developed in our laboratory. Superporous agarose beads are prepared by a double emulsification procedure and are characterised by two sets of pores,

*Corresponding author.

0021-9673/98/$19.00
PII S0021-9673(97)00953-9

normal diffusion pores and flow pores, or superpores. These superpores, whose diameter is a substantial fraction of the particle diameter (i.e. 1/3 to 1/10 of the particle diameter), allow part of the chromatographic flow to pass through each individual bead. This gives an improved mass transfer, especially in situations where diffusion is the limiting factor for the overall performance of a chromatographic separation [15,16].

The ability of the superporous agarose beads to reduce the effective diffusion distances for chromatographed substances is very dependent upon the ratio of the superpore fluid velocity to the interstitial fluid velocity. Thus, it is of great importance to know the flow characteristics within the superporous beads i.e. the intraparticle fluid velocity in comparison with the interstitial fluid velocity, the tortuosity of the superpores, the presence of interconnecting pores and/or the presence of dead-end pores. An attempt to measure intraparticle flow was made by Pfeiffer et al. [17] by studying gigaporous 30–50 μm particles (POROS-OH 50, PerSeptive Biosystems, Cambridge, MA) and measuring the volumetric flow of liquid and gas through the particles. However, these measurements were made on isolated, single particles rather than particles packed in a column. Pore flow was also directly demonstrated using single superporous agarose particles, although no quantitative measurements were made [15].

In the present study a different approach was taken. Instead of studying isolated beads in an artificial surrounding, the beads were observed in their natural environment, i.e. in a packed bed. Furthermore, fluid velocities within the pores and between the beads were directly measured by following the movement of micro-particles (dyed yeast cells, suspended in the mobile phase) with a microscope/video camera. The collected data were compared with data calculated from the Kozeny–Carman equation [18].

2. Theoretical model

Fig. 1 illustrates a superporous agarose particle with two sets of pores, diffusion pores (hatched areas) and flow pores. When such particles are used in a chromatographic bed, it is very likely that part of the chromatographic flow will be diverted through the particles. Using a simplified theoretical model based on the Kozeny–Carman equation [18], a rough approximation is made too see how much of the chromatographic flow can theoretically be expected to go through the particles.

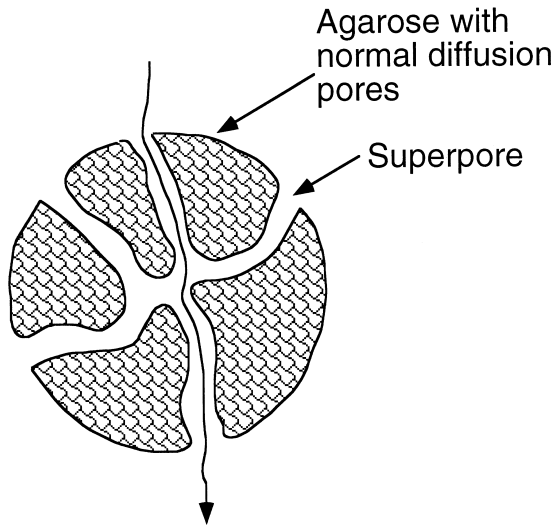

Fig. 1. Schematic picture of a superporous agarose particle.

The channels (interstitial pores) between the particles in a chromatographic bed may as a first approximation be considered hydraulically similar to the superpores inside the particles. According to Kozeny–Carman, the interstitial pores are considered to be tubeshaped. These tubes may have a physically complicated and varied cross-sectional area, but they are mathematically modeled as tubes having a constant hydraulic mean diameter (D_i). In the derivation of the Kozeny–Carman model, D_i is related to the particle size (D_p), and the bed porosity (ϵ), as in Eq. (1).

$$D_i = \frac{2D_p\epsilon}{3(1-\epsilon)} \quad (1)$$

Assuming an ϵ value of 0.4 (experimental value for a packed column of agarose beads with a particle size of 300–500 μm [15]) and substituting into Eq. (1) gives:

$$D_i = \frac{D_p}{2.25} \quad (2)$$

In a chromatography system, sufficient pumping energy has to be supplied in order to overcome the friction within the porous chromatography bed and to accelerate the fluid until it reaches the interstitial fluid velocity. This increased kinetic energy is dissipated completely when the fluid leaves the porous bed. However, in the present case, the fluid velocity is sufficiently low to neglect the kinetic energy loss relative to the friction energy loss. Thus, the total pressure drop is given by the Kozeny–Carman equation that can be expressed as:

$$\frac{\Delta p}{L} = \text{constant}\,\frac{\mu u}{(D_i)^2} \quad (3)$$

where $\Delta p/L$ is the pressure drop over the length of the bed, u is the mean pore velocity of the fluid, μ is the viscosity of the fluid and D_i is the hydraulic mean diameter of the interstitial pores. Since the same pressure gradient is formed over the superpores (D_s, defined as the mean diameter of the superpores), as over the interstitial pores (D_i), the flow distribution between the respective pores can easily be estimated from Eq. (3):

$$\text{Relative superpore fluid velocity (\% of interstitial pore fluid velocity)} = \left(\frac{D_s}{D_i}\right)^2 \times 100\% \quad (4)$$

The relative superpore fluid velocity is thus dependent upon the ratio between the square of the respective pore diameter. Combining Eqs. (2) and (4) gives:

$$\text{Relative superpore fluid velocity (\% of interstitial pore fluid velocity)} = 5.06\left(\frac{D_s}{D_p}\right)^2 \times 100\% \quad (5)$$

For an analysis of the flow distribution in the upper laminar region and in the turbulent region see Schlünder [19]. Table 1 gives the calculated particle pore fluid velocity (as % of interstitial pore fluid velocity) for different particle pore sizes, when $D_i = D_p/2.25$.

The calculated results in Table 1 illustrates why pore flow is not observed in practice using standard chromatography materials. These materials (agarose, silica, polystyrene, etc.) certainly possess a continuous network of pores, but the pores are too narrow. Even wide pore (300 Å) HPLC-grade silica (10 μm particle diameter) is calculated to exhibit insignificant pore fluid velocity, just 0.005% of the interstitial fluid velocity (Table 1). Standard agarose particles which have the same pore size (300 Å) but are ten times larger than the silica particles have a 100-fold lower pore fluid velocity.

Table 1
The calculated particle pore fluid velocity (as % of interstitial pore fluid velocity) for different particle pore sizes, when $D_i = D_p/2.25$

Pore size (as % of particle size)	30	20	10	3	1	0.3
Pore fluid velocity (as % of interstitial pore fluid velocity)	45.6	20.2	5.1	0.46	0.051	0.0046

3. Experimental

3.1. Materials

Agarose powder (Sepharose quality) was a gift from Pharmacia Biotech AB (Uppsala, Sweden). Polyoxyethylenesorbitanmonooleate (Tween 80) was obtained from Merck Schuchardt (Munich, Germany). Sorbitane trioleate (Span 85) was purchased from Fluka (Buchs, Switzerland). Cyclohexane (puriss.) was purchased from Merck (Darmstadt, Germany). Aniline blue (water soluble) was obtained from BDH chemicals (Poole, UK). Dextran T-500 was obtained from Pharmacia Biotech AB (Stockholm, Sweden). Baker's yeast (*Saccharomyces cerevisiae*) was obtained from AB Jästbolaget (Stockholm, Sweden).

3.2. Preparation of superporous agarose beads

Superporous agarose beads with an average superpore diameter of 30 μm (measured by observations under microscope) and a superpore porosity of 40% (defined by the method of preparation and verified by size exclusion experiments with 0.5 μm latex particles) were prepared as described previously [15]. The beads were wet-sized using graded metal screens

in the following particle size ranges, 106–180 μm, 180–300 μm and 300–500 μm.

3.3. Preparation of homogeneous agarose beads

The homogeneous agarose beads were prepared by emulsifying an agarose solution (6%, w/v) in cyclohexane containing Span 85 (4%, v/v), as described previously [15]. The beads were wet-sized using graded metal screens in the following particle size ranges, 106–180 μm, 180–300 μm and 300–500 μm. When slurry-packed in a column, all three particle size ranges gives columns with a porosity of 0.4.

3.4. Dyeing of yeast cells

The yeast cells used (Baker's yeast) were dyed with a 10% (v/v) aqueous lactic acid solution, containing 0.5% (w/v) aniline blue for 2 h and then washed with water. The dyed yeast cells appeared as dark blue bodies under the microscope.

3.5. Experimental set-up to measure superpore fluid velocities

The experimental set-up used for measuring superpore and interstitial pore fluid velocities is outlined in Fig. 2. The superporous beads that were studied were mixed with a 20-fold excess of homogeneous beads having the the same particle size, and slurry-packed in a special glass column (60×7 mm I.D.) with the center part (about 20 mm) having a squared cross-section (5×5 mm). Each end of the column was fitted with several nylon nets in order to retain the beads and to act as flow distributors, and a silicon stopper and Teflon tubing. The glass column was placed horizontally under a microscope (Nikon Labophot-2 light microscope; 4× or 10× objective lens). The microscope was focused on particles situated 4 layers down in the column. The condenser and diaphragm were adjusted to give a field of depth of about 200 μm with the 4× objective (used for the study of large beads) and about 60 μm with the 10× objective (used for the study of small beads). Dyed yeast cells suspended in 20% Dextran T-500 aqueous solution were then pumped through the column. The movement of the yeast cells was recorded with a standard VHS video camera (SALORA Cam corder SK 5800). The video recordings were then studied and the fluid velocities associated with a selected bead were calculated from the movement of the yeast cells within the superpores (U_s) and outside the bead (U_i). To this end the flow paths of the yeast cells were tracked and transferred from the monitor to transparent plastic sheets (OH-film) together with time information. Average values for U_s and U_i from approximately ten yeast cell flow paths were then calculated for each superporous agarose bead studied.

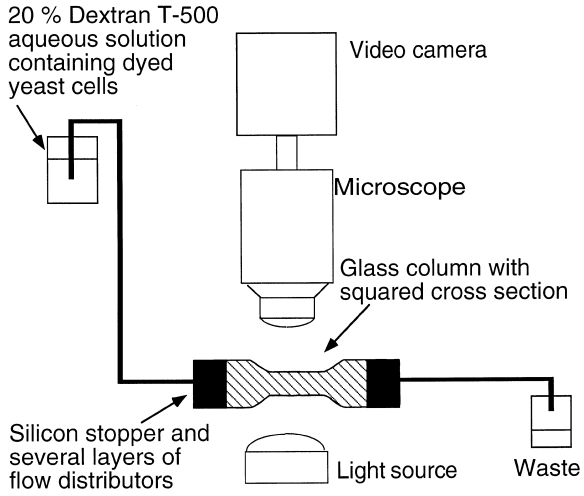

Fig. 2. Experimental set-up for measuring the superpore fluid velocity. Details are given in the experimental section.

4. Results and discussion

4.1. Considerations to make when measuring superpore fluid velocities

When measuring superpore fluid velocities in a packed column of superporous agarose beads, the measurements must be made several particle layers away from the column wall in order to avoid packing anomalies close to the wall. A distance of four particle layers into the column, corresponding to about 3.25 bead diameters as measured by microscopy, was considered sufficient. According to Benenati and Brosilow [20], the voidage fraction oscillates through several maxima and minima before

settling out at the mean voidage of about 4 bead diameters from a flat container wall for a packed bed of uniform spheres. When measuring velocities of the dyed yeast cells at this distance into the column, three important adjustments had to be made on the experimental conditions in order to improve the likelihood of seeing yeast cells as reasonably sharp spots under the microscope.

First, the focusing depth of the microscope had to be minimized by appropriately adjusting the condenser and the condenser diaphragm. In this manner, yeast cells at depths other than the bead under study became unfocused and almost invisible, thereby minimizing interference.

Secondly, a superporous bead contains many internal surfaces that refract light, making it considerably more opaque than a homogeneous bead. It was therefore difficult to observe yeast cells on the far side of a superporous bead. This problem was alleviated by diluting the superporous beads with a 20-fold excess of homogenous beads of the same particle size, thereby statistically securing an unobstructed view down to the fourth layer of beads.

Thirdly, the refractive index of the mobile phase was increased by adding 20% Dextran T-500 polymer. The polymer does not penetrate the normal agarose pores very well, allowing for a higher concentration in the interstitial pores and the superpores than in the agarose phase. This reduces the refractive index difference between agarose and the mobile phase and makes the whole column more transparent.

4.2. Supporting experiments to verify the validity of the pore fluid velocity measurements

As discussed above, Dextran T-500 was added to facilitate the observation of yeast cell movement in the interior of the bed. Because of the viscosity of Dextran solutions, it was important to verify that these solutions give the same ratio between superpore fluid velocity and interstitial fluid velocity (U_s/U_i) as that of normal mobile phases such as water and buffers. An obvious requirement would be that the dextran solution behaves as a Newtonian solution at the shear rates generated inside the bed and inside the superpores during the experiment. Several reports describe Dextran T-500 solutions as Newtonian, at least at moderately high shear rates [21,22]. However, no data were available for concentrations as high as 20%, necessitating additional rheological experiments.

Table 2
Dynamic viscosity of a 20% Dextran T-500 aqueous solution at various shear rates

Shear rate (s^{-1})	0.29	1.2	4.6	18.5	73	291
Viscosity (mPa)	96	110	115	118	117	117

Table 2 shows the dynamic viscosity of a 20% Dextran T-500 aqueous solution at various shear rates, measured with a Bohlin rheometric system (Bohlin Reologi, Lund, Sweden). Only a slight increase in viscosity was observed over the broad range of shear rates applied. This slight increase coincided with the change of torque element during the measurements and could very well be caused by this change. It was thus concluded that a 20% Dextran T-500 aqueous solution is also Newtonian.

The shear rates obtained in the superpores and in the interstitial pores can be approximately calculated using the following equation for the shear rate in a tube [23]:

$$\gamma = \frac{4Q}{\pi(a)^3} \tag{6}$$

where Q is the volumetric flow-rate in the tube and a is the radius of the tube. The measured fluid velocities in the superpores (15 μm radius as determined by microscopy of particles sliced with an ultrathome) were in the range of 0.01–0.5 cm min^{-1} giving shear rates in the range of 0.3 to 20 s^{-1}. The measured fluid velocities in the interstitial pores (32, 53 and 90 μm hydraulic mean radius as calculated from the particle diameter; see Table 7 below) were in the range of 0.25–3.3 cm min^{-1} giving shear rates in the range of 2 to 70 s^{-1}. Clearly, all of the shear rates experienced during the fluid velocity experiments fall within the range given in Table 2, justifying the use of a viscous mobile phase during the experiments.

A complementary experiment was made in which the fluid velocities were measured in a superporous bead using pure water as the mobile phase. The mobile phase was then changed to a 20% Dextran T-500 aqueous solution, and the fluid velocities were

again measured in the same bead to see if the ratio between the superpore fluid velocity and the interstitial fluid velocity had changed. Importantly, the same ratio was found in both cases, supporting the above conclusion that the use of a viscous mobile phase is justified. Due to the opaqueness of the column with water as the mobile phase, the comparison had to be made in the first particle layer.

In summary, it can be concluded that the viscous (and refractive index-improving) mobile phase used in the experiments did not alter the ratio between the superpore fluid velocity and the interstitial fluid velocity. Thus, the experimental data and the conclusions obtained using Dextran T-500 aqueous solutions should also be valid for standard mobile phases, such as non-viscous buffers.

4.3. Superpore fluid velocities

Fig. 3 gives an illustration of the information that was obtained directly from fluid velocity experiments using dyed yeast cells. The figure gives the position of a single yeast cell each second during its passage through a superporous agarose bead. The particular bead studied was situated four bead layers from the column wall. The other beads in the figure were approximately, but not exactly, in the same plane as the studied bead and consequently appeared slightly out of focus on the video recording. The figure was constructed from the video recording and is drawn to size (bead diameter 150 μm, superpore diameter 30 μm (not shown) and yeast cell diameter 4 μm). The yeast cell has a high velocity near position A, which is characteristic of the interstitial pores. In position B, the yeast cell slows down before entering a superpore. It has reached the stagnation point in front of the bead, characteristic of flow past a sphere. Inside the superpore system, the velocity of the yeast cell is fairly constant. However, at position C, the velocity is particularly low. This may simply be due to obstructions in the pore system, or may possibly be an expression of the natural fluctuating pore width caused by the constant branching of the three-dimensional pore network. Such fluctuations are evident from light microscopy and SEM studies of superporous gels [15]. However, the apparently low velocity at position C may also reflect the fact that the observations were made in two dimensions, while the particle is certainly capable of movement in three dimensions. Thus, the lower observed speed at position C could indicate that the pore at this position did not follow the plane of the paper, but instead curved out of it. The beads were studied with a microscope which was usually arranged to have a depth of field large enough to cover at least half the depth of the actual bead. As long as the yeast cells moved within this field of depth, their movements would appear to be two-dimensional. However, as can be seen from Fig. 3 and which will be discussed later, the two-dimensional pathway through the bead is fairly smooth without showing any dramatic deviations from the column axis. From symmetry arguments, the same qualities should be true for the three-dimensional path. Thus, it is more likely that the slow velocity at position C is due to a truly lower transport rate than to a sharp bend of the pore out of the plane of the paper. Finally, in position D, the yeast cell has left the superpore system and slowly accelerates to a high velocity at position E.

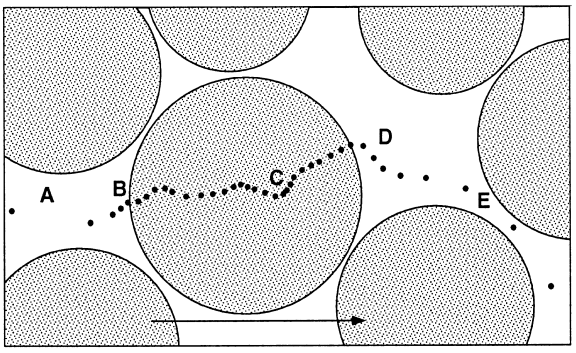

Fig. 3. The position of a dyed yeast cell passing through a superporous agarose bead (150 μm) at one second increments. The arrow indicates the longitudinal column direction. The fluid velocity in the experiment was 0.35 cm min^{-1} and the column inlet pressure was less than 0.05 bar.

The yeast cell positions that are shown in the figure were used to calculate the average superpore fluid velocity and the average interstitial pore velocity. When the superpore fluid velocity is expressed as percent of the interstitial pore velocity as in the tables below, the ratio is obtained from data using superpore paths and interstitial pore paths for the same bead, both paths being roughly parallel to each other.

Fig. 4 shows the observed two-dimensional flow

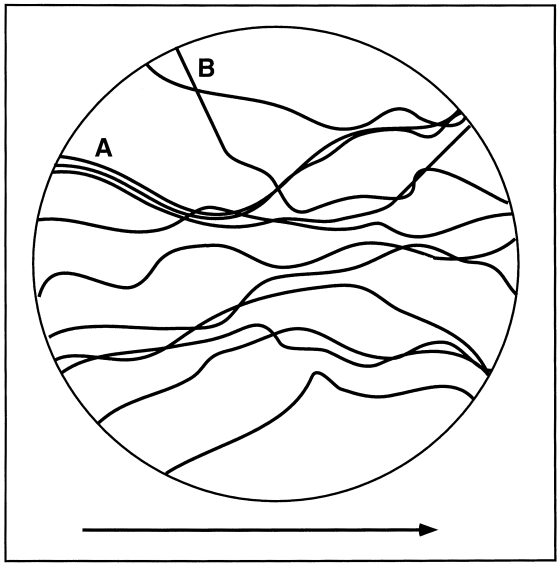

Fig. 4. The observed flow paths for 12 different yeast cells passing through a 300-μm superporous agarose bead. The arrow indicates the longitudinal column direction.

paths for 12 different yeast cells passing through one superporous bead. As can be seen, most flow paths are fairly straight, indicating an evenly distributed network of connecting superpores. Some of the tracks run very close to each other (e.g. at location A). This probably indicates that the corresponding yeast cells have followed the same set of superpores. Considering the fact that the bead diameter was 300 μm and that the superpore diameter was 30 μm, i.e. one tenth of the bead diameter, it is indeed very plausible that the closely running tracks belong to the same superpore.

Table 3 shows the measured two-dimensional tortuosities (τ) of the superpores and the interstitial pores for the three different particle size ranges investigated. In this case, the tortuosity is defined as the ratio of the actual length of the flow path to the shortest distance between the beginning and the end of the flow path. It is worth pointing out that this definition of tortuosity is the one used in chemical engineering and in physical chemistry, not the one used by chromatographers in connection with studies of column efficiency. The low tortuosity found in the superpores can be regarded as a quantitative measure of a well distributed network of interconnected flow pores in the beads. The travelling yeast particle will follow the pressure gradient through the bead, which should follow the column axis fairly closely. According to Fig. 4, there appears to be several alternative routes inside a particle which allow a cell to follow a flow path that is fairly parallel to the column axis. However, in some cases, the distribution of suitable flow pores seems to be less perfect, as can be seen by the flow path starting at position B in Fig. 4. Here the yeast cell is forced to follow pores that are far from parallel to the column axis.

Table 3 also shows simulated two- and three-dimensional tortuosities. The two- and three-dimensional flow paths were simulated using the spreadsheet program MS Excel. A random walk model was adopted, where it was assumed that the superpores are symmetrically distributed in the bead with no

Table 3
The measured two-dimensional tortuosities (τ) and simulated two- and three-dimensional tortuosities for the superpores and the interstitial pores. For each particle size range five particles were investigated

Pore type	Particle size range (μm)	Measured (2 dimensions)			Simulated (2 dimensions)			Simulated (3 dimensions)	
		n	τ	σ	m	τ	σ	τ	σ
Superpore	300–500	25	1.15	0.064	25	1.15	0.048	1.28	0.076
Superpore	180–300	25	1.12	0.026	25	1.12	0.025	1.23	0.034
Superpore	106–180	25	1.11	0.047	25	1.11	0.024	1.21	0.036
Interstitial	300–500	25	1.08	0.040	25	1.07	0.040	1.15	0.051
Interstitial	180–300	25	1.07	0.037		[a]			
Interstitial	106–180	25	1.08	0.040		[a]			

n = number of measurements, m = number of simulations, τ = mean tortuosity, σ = standard deviation.
[a] Due to the similar values of the measured interstitial pore tortuosities for the different particle sizes, only one set of simulations was needed, covering all three particle size ranges.

preferred direction, a reasonable assumption that is supported by microscopy observations. The passage of the yeast cells through both the superpores and the interstitial pores was modeled as a number of steps (usually about 50 for the superpores and about 10 for the interstitial pores), where each step involved a set of random additions in the X, Y and Z directions (X direction along the column axis; Y and Z perpendicular to the column axis). By making proper adjustments to the coefficients that modified these additions, two-dimensional flow paths were simulated that qualitatively had the same two-dimensional look as the experimentally obtained paths, as well as the same tortuosity and roughly the same standard deviation. Once the simulated and the experimentally determined two-dimensional tortuosity matched, the corresponding three-dimensional tortuosity was easily calculated. As can be seen in the table, the values for the three-dimensional tortuosities of the superpores are about 10% larger than those for the two-dimensional, while the interstitial pores show a 7% larger three-dimensional tortuosity. Thus, in order to obtain the true (three-dimensional) velocities, the measured intra- and interparticle velocities (two-dimensional) should be increased correspondingly.

It should be mentioned that the distances used for measuring the tortuosities of the interstitial pores were relatively short (approximately 2 to 3 bead diameters) in order to match the distances used for measuring the interstitial pore fluid velocities.

The three-dimensional tortuosities simulated here (both for the interstitial pores and the superpores), agree well with simulations made for diffusion in beds packed with solid spheres [24].

Table 4 shows the measured superpore fluid velocities and the corresponding interstitial pore fluid velocities for eleven superporous agarose beads in a column packed with beads that were fractionated to be in the size range 300–500 μm. As can be seen from the table, there is considerable fluctuation in the superpore fluid velocities observed for each single bead (fairly large standard deviations). A straightforward interpretation is that the superpore fluid velocity is dependent upon the intrinsic properties of the superpores as well as the environment of the individual particle, i.e. the pore properties and the pressure gradient in the interstitial pores surrounding the particle are locally varying. As also can be seen from the table, there is no correlation between individual particle sizes in the packed bed and the respective relative superpore fluid velocities, which suggests that the average pressure gradient over a particle is not dependent upon the size of the particle in a given bed. A closer inspection of Table 4 reveals that the ratio between the superpore fluid velocity and the interstitial fluid velocity seems to be independent of the interstitial fluid velocity. This conclusion is in agreement with the Kozeny–Carman equation.

Tables 5 and 6 give the same data as Table 4, but

Table 4
Fluid velocities in a bed packed with 300–500 μm particles

Bead #	D_p (μm)	Superpore measurements			Interstitial pore measurements			Relative velocity $V_s/V_i \times 100$ (%)
		n	V_s (cm/min)	σ (cm/min)	n	V_i (cm/min)	σ (cm/min)	
1	315	20	0.025	0.011	18	0.63	0.23	4.0
2	340	12	0.043	0.010	12	1.50	0.39	2.9
3	370	16	0.044	0.020	10	1.22	0.25	3.6
4	410	13	0.026	0.009	23	0.48	0.12	5.4
5	425	8	0.016	0.005	9	0.36	0.08	4.4
6	450	9	0.034	0.011	8	0.84	0.13	4.0
7	450	9	0.042	0.014	10	1.62	0.34	2.6
8	485	12	0.041	0.014	12	1.17	0.28	3.5
9	500	13	0.049	0.018	12	1.44	0.46	3.4
10	500	8	0.026	0.010	18	1.22	0.34	2.1
11	500	12	0.076	0.018	12	1.99	0.64	3.8

n = number of measurements, V_s = superpore fluid velocity, V_i = interstitial fluid velocity, σ = standard deviation.

Table 5
Fluid velocities in a bed packed with 180–300 μm particles

Bead #	D_p (μm)	Superpore measurements			Interstitial pore measurements			Relative velocity $V_s/V_i \times 100$ (%)
		n	V_s (cm/min)	σ (cm/min)	n	V_i (cm/min)	σ (cm/min)	
1	195	6	0.035	0.011	16	0.54	0.19	6.5
2	200	9	0.041	0.009	16	0.70	0.17	5.9
3	220	10	0.110	0.019	12	1.50	0.41	7.3
4	240	12	0.039	0.015	12	0.56	0.15	7.0
5	250	11	0.094	0.022	12	1.21	0.19	7.8
6	250	10	0.150	0.034	12	1.50	0.41	10.0
7	255	12	0.100	0.026	12	1.38	0.17	7.2
8	280	11	0.140	0.027	12	1.73	0.46	8.1
9	280	12	0.057	0.019	15	0.51	0.13	11.2
10	295	12	0.066	0.031	12	1.08	0.30	6.1
11	295	11	0.120	0.048	12	1.50	0.41	8.0
12	295	11	0.130	0.039	12	1.21	0.19	10.7
13	300	10	0.180	0.034	11	1.47	0.25	12.2

n = number of measurements, V_s = superpore fluid velocity, V_i = interstitial fluid velocity, σ = standard deviation.

for columns packed with superporous beads fractionated in the size range 180–300 μm and 106–180 μm, respectively. The same conclusions can be drawn from these two tables as from Table 4.

As seen in Tables 4–6 the relative superpore fluid velocities for 106–180 μm particles were 11–24% (average 17%), for 180–300 μm particles the relative velocities were 6–12% (average 7%) and for 300–500 μm particles the relative velocities were 2–5% (average 3%). These data agree well with the theoretically calculated values shown in Table 7.

However, the measured relative superpore fluid velocity values for the 106–180 μm fraction (17%) seems to be somewhat low compared to the corresponding theoretical value of 22%. This could possibly indicate that the bead preparation method that was used formed slightly narrower superpores for small particles. Another important conclusion from Tables 4–6 is that a chromatographic bed packed with smaller particles will have smaller interstitial pores with a higher flow resistance, thereby forcing a higher percentage of the total flow through the

Table 6
Fluid velocities in a bed packed with 106–180 μm particles

Bead #	D_p (μm)	Superpore measurements			Interstitial pore measurements			Relative velocity $V_s/V_i \times 100$ (%)
		n	V_s (cm/min)	σ (cm/min)	n	V_i (cm/min)	σ (cm/min)	
1	140	10	0.21	0.048	12	1.27	0.18	16.5
2	145	10	0.20	0.047	10	1.26	0.34	15.9
3	145	14	0.17	0.029	12	0.88	0.16	19.3
4	165	12	0.17	0.015	10	1.09	0.18	15.6
5	165	10	0.21	0.063	10	1.87	0.39	11.2
6	170	12	0.14	0.034	10	1.04	0.26	13.5
7	175	16	0.11	0.034	12	0.60	0.08	18.3
8	175	14	0.24	0.068	10	1.26	0.12	19.0
9	180	10	0.23	0.037	10	1.55	0.26	14.8
10	180	5	0.25	0.053	8	1.43	0.33	17.5
11	180	10	0.32	0.120	10	1.59	0.24	20.1
12	180	10	0.28	0.045	12	1.18	0.17	23.7

n = number of measurements, V_s = superpore fluid velocity, V_i = interstitial fluid velocity, σ = standard deviation.

Table 7
Calculated and measured superpore fluid velocity (as % of interstitial fluid velocity), for different particle size ranges

Particle size range (μm)	D_a (μm)	D_i[a] (μm)	D_s (μm)	Superpore fluid velocity (as % of interstitial fluid velocity)	
				Calculated[b] (%)	Observed (%)
300–500	400	178	30	2.8	3.3
180–300	240	107	30	7.9	7.3
106–180	143	64	30	22.2	17.4

[a] D_i is calculated using Eq. (1) in Section 2, with experimentally obtained values for the column porosity of 0.4 for all three particle size ranges.
[b] Calculations are based on the average particle diameter using the formula $(D_s/D_i)^2 \times 100\%$.
D_s = mean diameter of the superpores, D_i = hydraulic mean diameter of the interstitial pores, D_a = mean particle diameter.

superpores. This is again confirmed by the Kozeny–Carman model according to Eqs. (2) and (3).

The data in the tables describe the fluid velocities. It is also illustrative to calculate how much of the total flow actually passes through the superporous beads. Assuming a void fraction of 0.4 and a superpore fraction of 0.4, the ratio between the superpore flow-rate and the interstitial flow-rate would be 0.6 times the relative superpore fluid velocity ($(1–0.4)\times 0.4/0.4$). By using the experimental average values obtained from superpore fluid velocities in Table 7, it can be calculated that about 10% of the total volumetric flow goes through the superpores in a bed packed with 106–180 μm superporous particles. The corresponding values for the other beds would be as low as 4% and 2%.

4.4. Correction of obtained experimental data

The above section gives a large body of superpore fluid velocity data which, for instance, shows that the superpore fluid velocity in relation to interstitial pore fluid velocity may vary between 2% and 22%. All data refer to measurements on yeast cells, which raises the pertinent question of whether the data give a representative picture for convective transport that is equally applicable to small and large molecules, the situation encountered in a normal chromatography situation, or if corrections should be introduced.

The size of the yeast cells (2.5–5 μm) will tend to hinder their transport in the superpores. The hindrance factor has been estimated for the convection of neutral spheres in cylindrical pores, and becomes very significant when the particle diameter approaches the pore diameter [25]. Assuming an average superpore size of 30 μm, a hindrance factor of 0.95 is obtained [25] for the smallest yeast cells, and 0.8 for the largest yeast cells. The hindrance factor for transport in the interstitial pores, on the other hand, is insignificant even for the 106–180 μm particle bed, where the factor would be between 0.96 and 0.98. Thus, the data measured will slightly underestimate the superpore fluid velocity experienced by molecular species. On average, the superpore velocity should be increased by about 15%.

As the carrier fluid (20% Dextran T–500 aqueous solution) has almost the same density as the yeast cells, eventual deposition of yeast cells in the pores due to sedimentation was avoided completely.

Another point to consider is the fact that the experiments were carried out using packed beds containing a large excess of homogeneous beads (20:1) in order to improve the optical transparency of the bed. The flow pattern may be different around a homogeneous bead compared to a superporous bead. Clearly, the degree of pore flow in a studied bead could also be influenced by neighbouring superporous beads that would tend to diminish the pressure gradient in the interstitial pores close to the bead under study. These effects would certainly be most prominent in beds with high volumetric pore flow. The adopted experimental technique would then tend to overestimate the relative superpore fluid velocity. As mentioned in the preceeding section, the flow is overestimated by less than 10% for the 106–180-μm beads. (If all the beads were superpor-

ous the previous section demonstrated that, on average, 10% of the total flow would pass through the superporous beads. This would lower the pressure gradient in the interstitial pores with almost the same value and would give a correspondingly lower superpore fluid velocity). The overestimation for the other particle size ranges would be about 4% and 2% respectively.

All of the experimentally determined velocities have been two-dimensional velocities. The relative superpore fluid velocity, expressed as percent of the interstitial pore fluid velocity, is therefore also based on two-dimensional velocities. The purpose of the simulations used in one of the preceeding sections to obtain the three-dimensional tortuosities were to obtain an estimation of the error in measuring the two-dimensional velocities. These simulations showed that the true three-dimensional velocities should on average be approximately 10% and 7% higher for the superpores and the interstitial pores respectively. Thus, the two-dimensional data presented give a satisfactory description since the overall difference is only about 3%.

In summary it can be concluded that the directly obtained experimental data should give a reasonably accurate description of the relative fluid velocities. Justified corrections are small and partially cancel each other out.

5. Conclusions

We have directly measured convective pore fluid velocities in superporous agarose beads. The results are useful for describing the chromatographic performance of the beads, in spite of the fact that the experiments were based on studies of transported particles under conditions atypical for chromatography. However, complementary experiments as well as analysis of the experimental conditions support the notion that the data is representative for normal chromatography situations.

The superpore fluid velocities represented as % of interstitial fluid velocities were in the range of 2–5% for columns packed with 300–500 μm beads (3% average value), 6–12% for columns packed with 180–300 μm beads (7% average value) and 11–24% for columns packed with 106–180 μm beads (17% average value). The obtained data are in good agreement with a theoretical model based on the Kozeny–Carman equation.

The observed flow paths through the superporous particles were fairly straight (low tortuosity value), indicative of a well distributed superpore network.

The use of the large yeast cells particles to detect flow paths is suitable for wide pore materials such as superporous agarose. For other chromatography materials, much smaller particles and modified procedures should be used. A viable alternative could be sub-micron-sized latex particles in conjunction with fluorescence microscopy. Adoption of confocal microscopy techniques would also be an interesting prospect.

Acknowledgements

Dr. Helena Larsson at the Department of Food Technology is gratefully acknowledged for carrying out the dynamic viscosity measurements and for fruitful discussions.

Economic support from Pharmacia Biotech AB and The Swedish Center for Bioseparation is gratefully acknowledged.

References

[1] J.V. Dawkins, L.L. Lloyd, F.P. Warner, J. Chromatogr. 352 (1986) 157.
[2] L.L. Lloyd, F.P. Warner, J. Chromatogr. 512 (1990) 365.
[3] N.B. Afeyan, N.F. Gordon, I. Mazsaroff, L. Varady, S.P. Fulton, Y.B. Yang, F.E. Regnier, J. Chromatogr. 519 (1990) 1.
[4] S.P. Fulton, N.B. Afeyan, N.F. Gordon, F.E. Regnier, J. Chromatogr. 547 (1991) 452.
[5] G. Carta, M.E. Gregory, D.J. Kirwan, H.A. Massaldi, Sep. Technol. 2 (1992) 62.
[6] H. Komiyama, H. Inoue, J. Chem. Eng. Japan 7 (1974) 281.
[7] A. Nir, L.M. Pismen, Chem. Eng. Sci. 32 (1977) 35.
[8] A.E. Rodrigues, B.J. Ahn, A. Zoulalian, AIChE J. 28 (1982) 541.
[9] G.A. Heeter, A.I. Liapis, J. Chromatogr. A 761 (1997) 35.
[10] A.E. Rodrigues, Z.P. Lu, J.M. Loureiro, G. Carta, J. Chromatogr. A 653 (1993) 189.
[11] G. Carta, A.E. Rodrigues, Chem. Eng. Sci. 48 (1993) 3927.
[12] D.D. Frey, E. Schweinheim, C. Horváth, Biotechnol. Prog. 9 (1993) 273.

[13] Q. Li, E.W. Grandmaison, C.C. Hsu, D. Taylor, M.F.A. Goosen, Bioseparation 5 (1995) 189.
[14] P.-O. Larsson, PCT Int. Appl. WO 9319, 115.
[15] P.-E. Gustavsson, P.-O. Larsson, J. Chromatogr. A 734 (1996) 231.
[16] P.-E. Gustavsson, K. Mosbach, K. Nilsson, P.-O. Larsson, J. Chromatogr. A 776 (1997) 197.
[17] J.F. Pfeiffer, J.C. Chen, J.T. Hsu, AIChE J. 42 (1996) 932.
[18] J.M. Coulson, J.F. Richardson, J.R. Backhurst, J.H. Harker, Chemical Engineering, vol. 2, 4th ed., Pergamon Press, Oxford, 1991, pp. 132–136.
[19] E.U. Schlünder, Chem. Eng. Sci. 32 (1977) 845.
[20] R.F. Benenati, C.B. Brosilow, AIChE J. 8 (1962) 359.
[21] K.H. Kroner, H. Hustedt, M.-R. Kula, Biotech. Bioeng. 24 (1982) 1015.
[22] F. Tjerneld, S. Berner, A. Cajarville, G. Johansson, Enzyme Microb. Technol. 8 (1986) 417.
[23] H.A. Barnes, J.F. Hutton, K. Walters, An Introduction to Rheology, Elsevier Science Publishers, New York, p. 32.
[24] K.A. Akanni, J.W. Evans, I.S. Abramson, Chem. Eng. Sci. 42 (1987) 1945.
[25] W.M. Deen, AIChE J. 33 (1987) 1409.